

Perfectly matched layer for acoustic waveguide modeling — benchmark calculations and perturbation analysis

Ya Yan Lu¹ and Jianxin Zhu²

Abstract: The perfectly matched layer (PML) is a widely used technique for truncating unbounded domains in numerical simulations of wave propagation problems. In this paper, the PML technique is used with a standard one-way model to solve a benchmark problem for underwater acoustics modeling. Accurate solutions are obtained with a PML layer with a thickness of only a quarter of the wavelength. The effect of a PML is analyzed in a perturbation analysis for the Pekeris waveguide.

keyword: Perfectly matched layer, acoustic waveguides, one-way wave equations.

1 Introduction

As a simple model used in ocean acoustics [Jensen et al (2004); deSanto (1992); Frisk (1994)], the sea-bottom is approximated by an infinite fluid layer. In numerical simulations for sound waves in the ocean, for example using the Parabolic Equation (PE) method [Tappert (1977)] and the step-wise coupled mode method [Evans (1983)], the depth is usually truncated. To reduce spurious reflections from the lower bottom boundary (as a result of truncating the depth), an artificial absorbing layer [Tappert (1977); Evans (1983)] can be used. For some problems, a large truncation depth is needed to obtain a satisfactory solution when this technique is used. For PE models, the non-local transparent boundary conditions [Papadakis et al (1992); Arnold and Ehrhardt (1998); Yevick and Thomson (1999); Schmidt et al (2001)] can also be used. However, they require all the previous acoustic field along the bottom boundary in each marching step. The transparent boundary conditions cannot be used in the step-wise coupled mode method.

Yevick and Thomson (2000a) applied the perfectly matched layer (PML) technique [Berenger (1994); Chew

and Weedon (1994)] to PE models and demonstrated that PML is efficient at truncating the unbounded sea-bottom with minimal spurious reflections. The PML was originally introduced by Berenger (1994) for time domain electro-magnetic problems [Ha et al (2006); Hassan et al (2004)]. In the frequency domain, the PML corresponds to a complex coordinate stretching [Chew and Weedon (1994)]. The PML technique has been analyzed by the reflection of plane waves incident on the layer [Berenger (1994)]. The influence of a discretization on the reflection coefficient has been studied by Yevick et al (1997).

In section 3, we provide new numerical evidence that the PML technique is truly effective at truncating the unbounded sea-bottom. Previous numerical results in Yevick and Thomson (2000a) are based on the classical PML and for range-independent problems. We apply the modified PML [Chen et al (1995); Fang and Wu (1995)] in a wide-angle PE model to solve a range-dependent benchmark problem (wedge with penetrable bottoms) [Jensen and Ferla (1990)]. Accurate solutions are obtained by truncating the depth to 215 m, where the maximum depth of the water column is 200 m and the thickness of PML is 15 m (a quarter of the wavelength). These numerical results indicate that the PML is much more effective than artificial absorbing layers.

The objective of section 4 is to develop a theoretical understanding of the PML technique concerning its application for waveguides. Previous theoretical results on reflection coefficients of the PML are not sufficient for waveguide problems where a large distance in the propagation direction is involved. A small reflection coefficient cannot guarantee that the solution is still reliable after propagating a large distance. Our approach is to find out how the modes of a simple waveguide are modified by a PML. We develop a perturbation theory for normal modes in waveguides terminated below by a PML. Our theory reveals that the originally real horizontal wavenumber of a trapped mode (in a lossless waveguide) may become complex leading to possible instabil-

¹ Department of Mathematics, City University of Hong Kong, Kowloon, Hong Kong.

² Department of Mathematics, Zhejiang University, Hangzhou, China

ity or non-physical attenuation of the mode. Therefore, the PML parameters must be chosen carefully if the total propagation distance is large.

2 The PML and its reflection coefficient

We consider the two dimensional Helmholtz equation:

$$\rho \frac{\partial}{\partial x} \left(\frac{1}{\rho} \frac{\partial u}{\partial x} \right) + \rho \frac{\partial}{\partial z} \left(\frac{1}{\rho} \frac{\partial u}{\partial z} \right) + k^2 u = 0, \quad (1)$$

where x is the horizontal distance (called range in ocean acoustics), z is the depth, ρ is the density and k is the wavenumber. Both ρ and k are functions of x and z . For ocean acoustics, the pressure-release condition $u = 0$ is typically used at $z = 0$. If the ocean bottom is modeled by an infinite fluid layer, equation (1) is valid for the half plane $z > 0$. To use the PML, we need to assume that the medium is homogeneous for a sufficiently large depth. That is, we have some G , such that $\rho = \rho_2$ and $k = k_2$ for $z > G$, where ρ_2 and k_2 are constants.

The PML corresponds to changing the depth z to the complex variable \hat{z} [Chew and Weedon (1994)]:

$$\hat{z} = z + i \int_0^z \sigma(\tau) d\tau \quad (2)$$

where $\sigma(z) = 0$ for $0 < z \leq H$, $\sigma(z) > 0$ for $z > H$ and $H \geq G$. If we replace ∂_z in (1) by $\partial_{\hat{z}} = [1 + i\sigma(z)]\partial_z$, we obtain the following modified Helmholtz equation:

$$\rho \frac{\partial}{\partial x} \left(\frac{1}{\rho} \frac{\partial u}{\partial x} \right) + \frac{\rho}{1 + i\sigma} \frac{\partial}{\partial z} \left(\frac{1}{\rho(1 + i\sigma)} \frac{\partial u}{\partial z} \right) + k^2 u = 0. \quad (3)$$

Notice that (1) and (3) are different only if $z > H$. For numerical computations, it is necessary to truncate the variable z to a finite interval, say $0 < z < D$, where $D > H$. The interval (H, D) is then the actual PML layer. Equation (3) is solved with a suitable boundary condition at $z = D$. In the simplest case, we let

$$u = 0 \quad \text{at} \quad z = D. \quad (4)$$

Alternatively, we can assume

$$u_z = a u \quad \text{at} \quad z = D \quad (5)$$

for some constant a .

Standard analysis [Berenger (1994)] of the PML is concerned with the reflection of a down-going plane wave incident upon the interface at $z = H$. In the vicinity of

$z = H$, the density and wavenumber are constants and the Helmholtz equation is simplified to $u_{xx} + u_{zz} + k_2^2 u = 0$. For $G < z < H$, we consider a down-going (towards $z = +\infty$) plane wave solution

$$u^{(d)} = e^{i(\alpha x + \beta z)},$$

where $\beta > 0$ and $\alpha^2 + \beta^2 = k_2^2$. For the original Helmholtz equation (1), the above solution is extended to $z > H$ without any reflections. For the modified equation (3), the incident wave $u^{(d)}$ above is connected to

$$u^{(d)} = e^{i(\alpha x + \beta \hat{z})} = e^{i(\alpha x + \beta z)} e^{-\beta \int_0^z \sigma(\tau) d\tau} \quad \text{for} \quad z > H.$$

With $\sigma(z) > 0$ for $z > H$, if $\int_0^z \sigma(\tau) d\tau \rightarrow \infty$ as $z \rightarrow \infty$, then $u^{(d)}(x, z) \rightarrow 0$ as $z \rightarrow \infty$. Therefore, the radiation condition for the Helmholtz equation is equivalent to the condition

$$\lim_{z \rightarrow \infty} u = 0 \quad (6)$$

for the modified equation (3). In practice, the PML has a finite thickness and a boundary condition is imposed at $z = D$. If the zero Dirichlet condition (4) is used, we have the following solution of (3):

$$u = u^{(d)} + u^{(u)} = e^{i(\alpha x + \beta \hat{z})} + R e^{i(\alpha x - \beta \hat{z})} \quad \text{for} \quad z > H,$$

where

$$R = -e^{2i\beta D} e^{-2\beta \int_H^D \sigma(\tau) d\tau}.$$

Notice that $|R| = \exp(-2\beta \int_H^D \sigma(\tau) d\tau)$, thus the reflection coefficient is exponentially small with $\int_H^D \sigma(\tau) d\tau$, but it also depends the angle of incidence. Let θ be the angle between the z axis and the wave vector (α, β) , we have $\beta = k_2 \cos(\theta)$. Therefore, the reflection coefficient is smallest for pure down-going waves ($\theta = 0$). When θ is close to $\pm\pi/2$, β is small and the reflection coefficient is relatively large. One observation is that $|R|$ depends on the integral $\int_H^D \sigma(\tau) d\tau$, rather than on $|H - D|$. Therefore, if a larger σ is used, the thickness of the PML can be reduced while keeping the magnitude of the reflection coefficient unchanged. In reality, when the z variable is discretized in a numerical scheme, the truncation error may be dominant. Therefore, $|H - D|$ cannot be too small. A study of the reflection coefficient including the effect of discretizing z can be found in Yevick et al (1997). Furthermore, when the Helmholtz equation is solved with some numerical method, it is natural to require that the reflection coefficient is as small as the errors introduced in the discretization of the domain. For example, when a

second order finite difference method is used, we could require that

$$e^{-k_2 \cos(\theta_*) \int_H^D \sigma(\tau) d\tau} \sim \left(\frac{\Delta z}{\lambda} \right)^2,$$

where $\lambda = 2\pi/k_2$ is the wavelength in the homogeneous sea-bottom, Δz is the grid size in z and θ_* is the maximum angle of incidence for which an accurate solution is needed.

The above reflection coefficient analysis is actually incomplete, since waves that decay in the positive z direction are not considered. For a range-independent waveguide (i.e. ρ and k are independent of x), we have the trapped modes given in the form

$$u^{(d)} = e^{i\alpha x - \gamma(z-H)}$$

for $z > G$, where $\gamma > 0$ and $\alpha^2 - \gamma^2 = k_2^2$. The solution decays exponentially in the positive z direction. With the transform $z \rightarrow \hat{z}$, the solution still decays exponentially in z and it is consistent with condition (6). When the PML is truncated at $z = D$ with the boundary condition (4), the solution of (3) for $z > H$ is now given by

$$u = u^{(d)} + u^{(u)} = e^{i\alpha x - \gamma(\hat{z}-H)} + R e^{i\alpha x + \gamma(\hat{z}-H)}$$

for

$$R = -e^{-2\gamma(D-H+i \int_H^D \sigma(\tau) d\tau)}.$$

Here, we have defined the reflection coefficient relative to the solution at $z = H$, therefore, H is involved in the formula of R . Since $|R| = e^{-2\gamma(D-H)}$, we can see that the magnitude of the reflection coefficient is independent of σ . In order to reduce the reflection, we could increase D . Alternatively [Chen et al (1995); Fang and Wu (1995)], we can include a new term in the real part of \hat{z} :

$$\hat{z} = z + \int_0^z [\gamma(\tau) + i\sigma(\tau)] d\tau, \quad (7)$$

where $\gamma(z) = 0$ for $z \leq H$ and $\gamma(z) > 0$ for $z > H$. In this case, the formula of R can be easily obtained by replacing σ with $\sigma - i\gamma$.

3 Application of PML to a benchmark problem

Yevick and Thomson (2000a) applied the PML technique to the PE method. They compared the PML method with the artificial absorbing layer technique for a number of

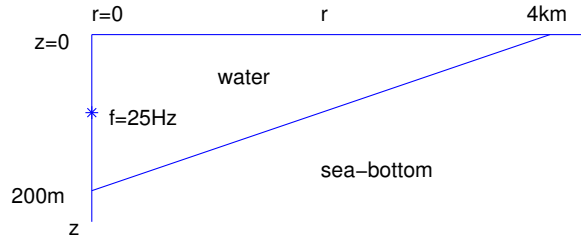


Figure 1 : Benchmark wedge problem with a penetrable sea-bottom.

range-independent problems. In this section, we consider a range-dependent benchmark problem — wedge with a penetrable bottom [Jensen and Ferla (1990)]. As shown in Fig. 1, the problem is concerned with a homogeneous water column (sound speed $c = 1500 m/s$, density $\rho = 1 g/cm^3$) above a homogeneous sea-bottom ($c = 1700 m/s$, $\rho = 1.5 g/cm^3$), the water-bottom interface is a linear function of the radial variable r which has a maximum of 200 m at $r = 0$ and it reaches zero at $r = 4000$ m. A point source of frequency $f = 25$ Hz is located at $r = 0$ and $z = 100$ m.

For this problem, the maximum depth of the water column is 200 m. Previous PE solutions [Jensen and Ferla (1990); Thomson (1990); Collins (1990)] of this benchmark problem based on artificial absorbing layers typically use a total depth of 2000 m to 4000 m. When a transparent boundary condition is used with a wide-angle PE model [Yevick and Thomson (1999)], a very small total depth is possible. With a PML, we obtain accurate results by truncating the depth at 215 m. The thickness of the PML is only 15 m. Since the frequency is 25 Hz, this corresponds to a quarter of the wavelength. Compared with the transparent boundary condition method, the PML technique is much easier to implement.

For PE modeling of a point source in a radially symmetric medium, the Helmholtz equation (1) is regarded as the far field equation, where x is now replaced by the radial variable r , i.e., the horizontal distance to the source. For a given reference wavenumber k_0 and the function ϕ defined in $u = \phi e^{ik_0 r}$, the far field equation is further approximated by the following one-way Helmholtz equation:

$$\frac{\partial \phi}{\partial r} = ik_0 \left[\sqrt{1 + X(r)} - 1 \right] \phi, \quad (8)$$

where $X(r)$ is the operator defined by

$$X(r) = \frac{\rho}{k_0^2} \frac{\partial}{\partial z} \left(\frac{1}{\rho} \frac{\partial}{\partial z} \right) + \frac{k^2}{k_0^2} - 1, \quad (9)$$

where k and ρ are functions of r and z . This equation must be supplemented with a suitable starting field at $r = 0$. For a step from r_j to $r_{j+1} = r_j + \Delta r$, Eq. (8) is formally discretized as

$$\phi_{j+1} = P\phi_j, \quad P = P(X_{j+1/2}) = e^{is(\sqrt{1+X_{j+1/2}}-1)}, \quad (10)$$

where $s = k_0\Delta r$, $X_{j+1/2}$ is X evaluated at $r_j + \Delta r/2$, ϕ_j approximates ϕ at r_j , etc. If $P(X)$ is approximated by a rational function of X [Collins (1993b)],

$$P(X) \approx a_0 + \sum_{l=1}^p \frac{a_l}{X + b_l}, \quad (11)$$

where p is a positive integer, a_0, a_1, b_1, \dots are coefficients that depend on both s and p , then ϕ_{j+1} can be evaluated as

$$\phi_{j+1} = a_0\phi_j + \sum_{l=1}^p a_l w_l, \quad (12)$$

where w_l must be solved from

$$(X_{j+1/2} + b_l) w_l = \phi_j. \quad (13)$$

PE solutions of the benchmark wedge problem were obtained by Jensen and Ferla (1990), Thomson (1990) and Collins (1990). These PE results are consistent with each other, they are roughly consistent with the one-way coupled mode solution [Jensen and Ferla (1990)] which approximates (8) better. The PE results are not satisfactory when compared with the full two-way coupled mode solution [Jensen and Ferla (1990)]. This has led to the development of improved one-way models [Porter et al (1991)] using energy-conserving corrections [Collins and Westwood (1991); Collins (1993a)] or the single scatter approximation [Lu and Ho (2002a); Ho and Lu (2003)]. Since the purpose of the present work is to demonstrate the capability of the PML, we will not consider these improved one-way models. All three PE solutions [Jensen and Ferla (1990); Thomson (1990); Collins (1990)] are calculated with the grid sizes $\Delta r = 5$ m and $\Delta z = 1$ m and the reference wavenumber $k_0 = 2\pi f/c_0$, where $c_0 = 1500$ m/s. The Greene's starting field [Greene (1984)] is used in Jensen and Ferla

(1990) and Collins (1990). Thomson and Bohun's starting field [Thomson and Bohun (1988)] is used in Thomson (1990). In the following, we use the same Δr , Δz , k_0 and Greene's starting field. The implicit finite difference PE solutions in Jensen and Ferla (1990) and Thomson (1990) are based on the wide-angle PE model of Claerbout and the Crank-Nicolson scheme for discretizing r . This is identical to the [1/1] Padé approximant of P :

$$P(X) \approx \frac{1 + \bar{e}_1 X}{1 + e_1 X}, \quad e_1 = \frac{1}{4} - \frac{is}{4}, \quad (14)$$

and it can be written as (11) for $p = 1$ and

$$a_0 = \frac{1 + si}{1 - si}, \quad a_1 = \frac{-8si}{(1 - si)^2}, \quad b_1 = \frac{4}{1 - si}.$$

PE solutions based on higher order Padé approximants are also calculated in Collins (1990), but they are close to the solution based on (14). In the following, we will only consider the [1/1] Padé approximant (14).

In the case of a lossless bottom, artificial attenuation is used in the PE calculations [Jensen and Ferla (1990); Thomson (1990); Collins (1990)]. In Thomson (1990), the artificial attenuation is linearly increased from zero at $z = 512$ m to 2 dB/ λ at $z = 2048$ m and the depth is terminated at $D = 2048$ m with a pressure release boundary condition. We repeated this calculation and obtained a solution which is denoted as AA1. In Jensen and Ferla (1990) and Collins (1990), the depth is truncated at $D = 4000$ m. We did a similar calculation with an artificial attenuation increased linearly from zero at 1500 m to 2 dB/ λ at $z = 4000$ m. The latter solution will be denoted by AA2 and it serves as our reference solution. In Fig. 2, the solution AA2 is shown as the solid curves. The transmission loss curve at $z = 150$ m exhibits some oscillations as in the original works [Jensen and Ferla (1990); Thomson (1990); Collins (1990)]. The one-way coupled mode solution [Jensen and Ferla (1990)] which solves the one-way Helmholtz equation (8) more accurately does not have these oscillations. Presumably, these oscillations are caused by evanescent modes excited by the staircase approximation of the sloping interface. The [1/1] Padé approximant (14) is an unitary operator which incorrectly propagates the evanescent modes. These oscillations can be removed if the one-way propagator P is properly approximated by a rational approximant that can suppress the evanescent modes [Milinazzo et al (1997); Lu (1998); Yevick and Thomson (2000b); Lu and Ho (2002b); Chui and Lu (2004)].

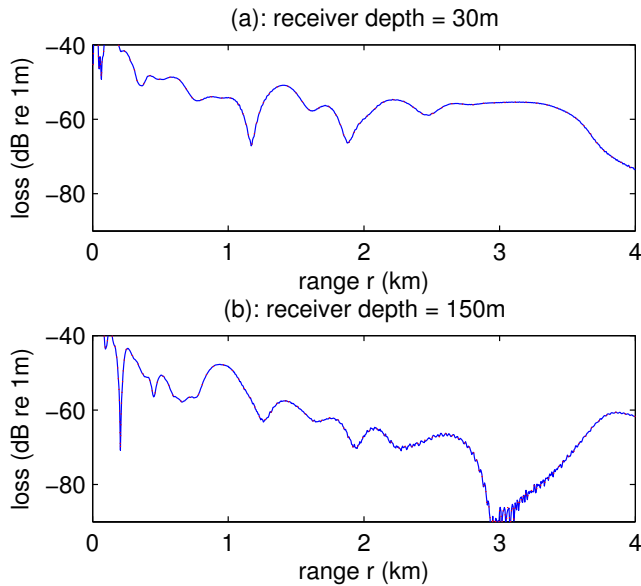


Figure 2 : Propagation losses versus range for the lossless penetrable wedge. Wide-angle PE predictions based on an artificial absorbing layer (solution AA2 obtained with $D = 4000$ m shown as the solid curves) and a PML (solution PML1 obtained with $D = 215$ m shown as the dots) are compared. The solid curve and the dotted curve are nearly identical.

When the PML is used, the operator X is modified as

$$X(r) = \frac{\rho}{k_0^2 \eta} \frac{\partial}{\partial z} \left(\frac{1}{\rho \eta} \frac{\partial}{\partial z} \right) + \frac{k^2}{k_0^2} - 1, \quad (15)$$

where $\eta = 1 + \gamma(z) + i\sigma(z)$ for γ and σ defined in (7). The actual PML layer is $H < z < D$. We have $\eta = 1$ for $z \leq H$. In the following, we set $H = 200$ m, $D = 215$ m and

$$\sigma(z) = \frac{200\tau^3}{1 + \tau^2}, \quad \gamma(z) = \frac{100\tau^3}{1 + \tau^2}, \quad \tau = \frac{z - H}{D - H}.$$

The depth z is terminated at $z = D$ with the boundary condition $u = 0$ at $z = D = 215$ m. The numerical solution with this choice of the PML will be denoted as PML1 and it is shown as the dotted curves in Fig. 2. The two curves in Fig. 2 can hardly be distinguished, therefore, PML1 has a good agreement with the reference solution AA2. In fact, the solution PML1 is even more accurate than AA1 (obtained with $D = 2048$ m). This can be observed in Fig. 3 where the errors in transmission loss are plotted for both PML1 and AA1, assuming that the reference solution AA2 is exact.

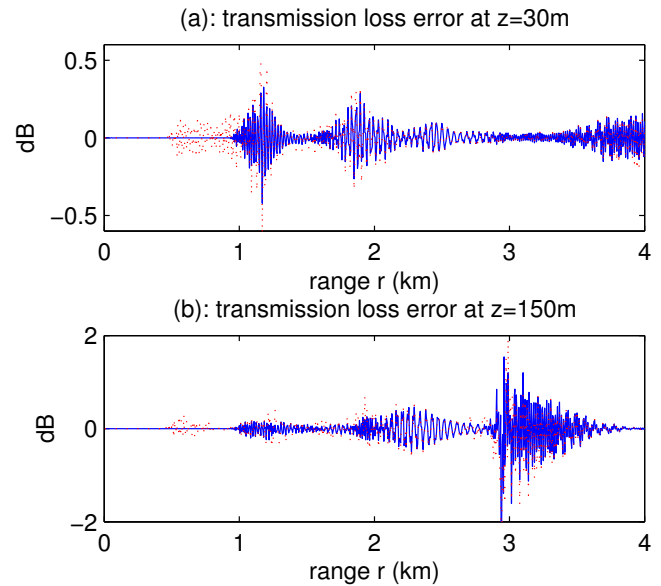


Figure 3 : Errors in wide-angle PE transmission loss predictions for lossless penetrable wedge, assuming that the solution AA2 (obtained with an artificial absorbing layer and a maximum depth of $D = 4000$ m) is exact. The differences between AA2 and PML1 (obtained with a PML and $D = 215$ m) are shown as the solid curves. The differences between AA2 and AA1 (obtained with an artificial absorbing layer and $D = 2048$ m) are shown as the dots.

For the benchmark wedge problem with a lossy bottom, we have a constant attenuation of 0.5 dB/ λ for the bottom. In the first calculation, we follow Thomson (1990) and let artificial attenuation increase linearly from 0.5 dB/ λ at $z = 512$ m to the maximum of 2 dB/ λ at $z = 2048$ m. The bottom is then terminated at $z = D = 2048$ m with a pressure-release boundary condition. The obtained solution is denoted as AA3. The problem with a lossy bottom is easier compared with the earlier case of the lossless bottom. In Jensen and Ferla (1990) and Collins (1990), the depth z is terminated at $D = 2000$ m. To get a definite reference solution, we use $D = 4000$ m as before and let attenuation to increase linearly from the original value of 0.5 dB/ λ at $z = 1500$ m to the maximum value of 2 dB/ λ at $z = D = 4000$ m. The obtained solution serves as our reference solution and it is denoted as AA4. For the PML calculation, the same parameters are used. The obtained solution, denoted by PML2, is shown in Fig. 4 together with the reference solution AA4. It is clear that these two solutions are nearly identical.

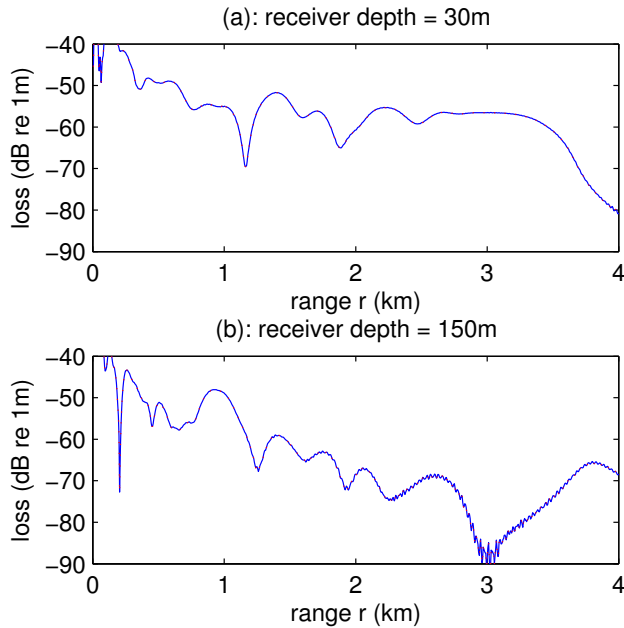


Figure 4 : Propagation losses versus range for the lossy penetrable wedge. Wide-angle PE predictions based on an artificial absorbing layer (solution AA4 obtained with $D = 4000$ m shown as the solid curves) and a PML (solution PML2 obtained with $D = 215$ m shown as the dots) are compared.

The errors in the transmission loss are shown in Fig. 5, assuming that AA4 is exact. We observe that PML2 is more accurate than AA3.

It is natural to ask whether an acceptable solution can be obtained with a much smaller total depth D when an artificial absorbing layer is used. In the following, we let the artificial attenuation to increase linearly from $0.5 \text{ dB}/\lambda$ at $z = 300$ m to the maximum a_{max} at $z = D = 500$ m, where a_{max} is a parameter. We have varied a_{max} from $1 \text{ dB}/\lambda$ to $20 \text{ dB}/\lambda$ with an increment of $1 \text{ dB}/\lambda$ for each step. Using the reference solution AA4, we calculate the errors in transmission loss as before. In Fig. 6, the maxima (range from $r = 0$ to $r = 4000$ m) of these errors are shown for each a_{max} . It appears that the best choice of a_{max} depends on the receiver depth. At $z = 30$ m, the most accurate solution is obtained when $a_{max} = 10$. In this case, the largest error in transmission loss is about 0.4 dB . If the receiver is at $z = 150$ m, the most accurate solution is obtained when $a_{max} = 5$ and the maximum error is about 4 dB . In all cases, these solutions are clearly less accurate than the PML solution obtained with $D = 215$ m.

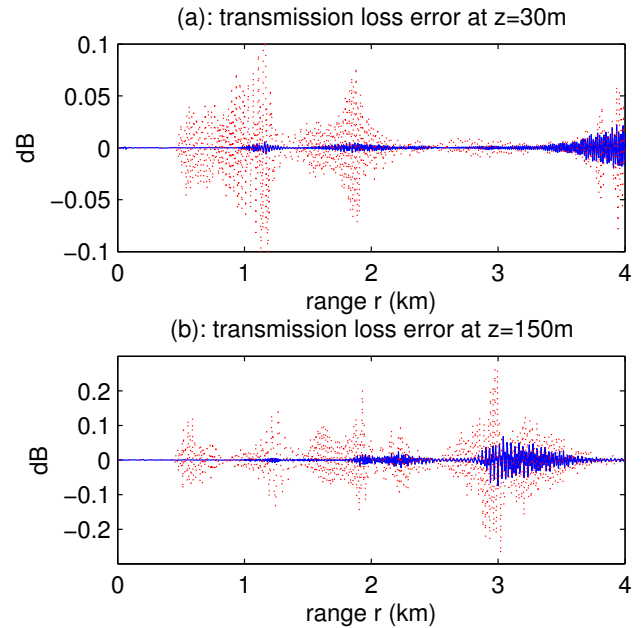


Figure 5 : Errors in wide-angle PE transmission loss predictions for lossy penetrable wedge, assuming that the solution AA4 (obtained with an artificial absorbing layer and a maximum depth of $D = 4000$ m) is exact. The differences between AA4 and PML2 (obtained with a PML and $D = 215$ m) are shown as the solid curves. The differences between AA4 and AA3 (obtained with an artificial absorbing layer and $D = 2048$ m) are shown as the dots.

4 Perturbation analysis

The reflection coefficient formula of a PML given in section 2 does not reveal how the solutions of the original Helmholtz equation (1) and the modified Helmholtz equation (3) differ. This is especially important for waveguide problems, since we are interested in the solution over a large range distance. The relatively small side-effects introduced by the PML may accumulate over a large range distance leading to a significant error in the solution. This has motivated us to study the effect of the PML on normal modes in a range-independent waveguide.

Consider a trapped mode, $\phi(z)e^{i\beta x}$, of the acoustic waveguide.

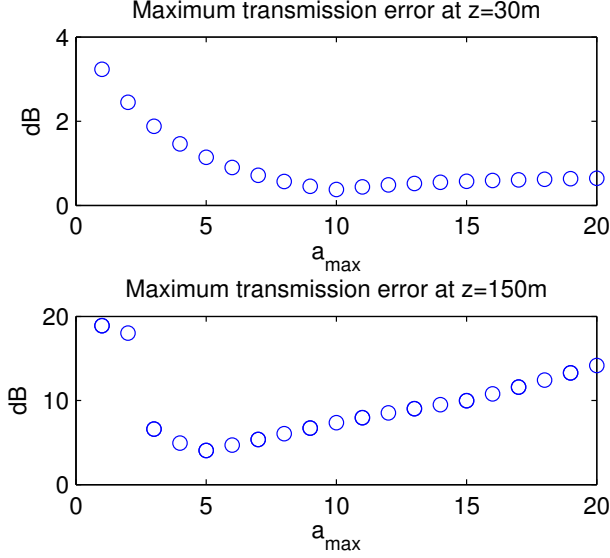


Figure 6 : Maximum errors in transmission loss versus a_{max} based on a wide-angle PE model and a linear artificial attenuation profile from $0.5 \text{ dB}/\lambda$ at $z = 300 \text{ m}$ to a_{max} at $z = D = 500 \text{ m}$. The bottom is terminated with a pressure-release condition at $z = D$. The errors are calculated assuming that the solution AA4 (obtained with an artificial absorbing layer and a maximum depth of $D = 4000 \text{ m}$) is exact.

uide satisfying the following eigenvalue problem

$$\rho \frac{d}{dz} \left(\frac{1}{\rho} \frac{d\phi}{dz} \right) + k^2 \phi = \beta^2 \phi \quad \text{for } z > 0, \quad (16)$$

$$\phi(0) = 0, \quad (17)$$

$$\lim_{z \rightarrow \infty} \phi(z) = 0. \quad (18)$$

For $z > G$, we assume that the wavenumber and the density are constants:

$$k(z) = k_2, \quad \rho(z) = \rho_2.$$

To satisfy condition (18), we must have $\lambda = \beta^2 > k_2^2$ and ϕ should decay to zero (as $z \rightarrow \infty$) like $e^{-\sqrt{\lambda - k_2^2} z}$. This gives rise to

$$\phi_z = i\sqrt{k_2^2 - \lambda} \phi \quad \text{for } z > G,$$

where the square root follows the standard definition, such that the square root of a negative number is a pure imaginary number with a positive imaginary part. This

allows us to reduce the original eigenvalue problem to a nonlinear eigenvalue problem on the finite interval $0 < z < H$, where $H > G$. It is

$$\rho \frac{d}{dz} \left(\frac{1}{\rho} \frac{d\phi}{dz} \right) + k^2 \phi = \lambda \phi \quad \text{for } 0 < z < H, \quad (19)$$

$$\phi = 0 \quad \text{at } z = 0, \quad (20)$$

$$\phi_z - i\sqrt{k_2^2 - \lambda} \phi = 0 \quad \text{at } z = H. \quad (21)$$

If we multiply equation (19) by $\rho^{-1} \bar{\phi}$ and integrate over $(0, H)$, we obtain

$$\begin{aligned} \lambda \int_0^H \frac{1}{\rho} |\phi|^2 dz - \int_0^H \frac{1}{\rho} k^2 |\phi|^2 dz \\ = \frac{1}{\rho(H)} i\sqrt{k_2^2 - \lambda} |\phi(H)|^2 - \int_0^H \frac{1}{\rho} |\phi_z|^2 dz. \end{aligned} \quad (22)$$

Let λ be a real eigenvalue of the system (19-21), from (22), we conclude that $i\sqrt{k_2^2 - \lambda}$ must be real, thus $\lambda \geq k_2^2$. Furthermore, the two terms in the right hand side of (22) are negative, therefore

$$\lambda \int_0^H \frac{1}{\rho} |\phi|^2 dz < \int_0^H \frac{1}{\rho} k^2 |\phi|^2 dz.$$

This gives rise to $\lambda < k_1^2$, where $k_1 = \max k(z)$.

The system (19-21) also has complex eigenvalues corresponding to the leaky modes of the waveguide. Since the branch-cut of the standard square root is the negative real axis, we have $\text{Re}(k_2^2 - \lambda)^{1/2} > 0$ if λ is complex with a non-zero imaginary part. Comparing the imaginary parts of the two sides of (22), we have $\text{Im} \lambda > 0$. Therefore, a leaky mode (which depends on x as $e^{i\sqrt{\lambda} x}$) decays exponentially in the propagation direction x .

When the PML is used, we have the following eigenvalue problem

$$\frac{\rho}{1 + i\sigma} \frac{d}{dz} \left(\frac{1}{\rho(1 + i\sigma)} \frac{d\tilde{\phi}}{dz} \right) + k^2 \tilde{\phi} = \tilde{\lambda} \tilde{\phi} \quad (23)$$

for $0 < z < D$ and

$$\tilde{\phi} = 0 \quad \text{at } z = 0, \quad (24)$$

$$\tilde{\phi} = 0 \quad \text{at } z = D, \quad \text{or} \quad (25)$$

$$\frac{d\tilde{\phi}}{dz} - a\tilde{\phi} = 0 \quad \text{at } z = D, \quad (26)$$

corresponding to the boundary conditions (4) or (5), respectively. For $z > G$, Eq. (23) is simplified to

$$\frac{d^2\tilde{\Phi}}{dz^2} + k_2^2\tilde{\Phi} = \tilde{\lambda}\tilde{\Phi}.$$

We can write down the solution as

$$\tilde{\Phi}(z) = C_1 e^{i\sqrt{k_2^2 - \tilde{\lambda}}(z-H)} + C_2 e^{-i\sqrt{k_2^2 - \tilde{\lambda}}(z-H)} \quad \text{for } z > G$$

where C_1 and C_2 are constants. This gives rise to

$$\frac{d\tilde{\Phi}}{dz} = q(\tilde{\lambda})\tilde{\Phi} \quad \text{at } z = H, \quad (27)$$

where

$$q(\tilde{\lambda}) = i\sqrt{k_2^2 - \tilde{\lambda}} \frac{1 + r(\tilde{\lambda})\varepsilon(\tilde{\lambda})}{1 - r(\tilde{\lambda})\varepsilon(\tilde{\lambda})},$$

for

$$\varepsilon(\tilde{\lambda}) = e^{2i\sqrt{k_2^2 - \tilde{\lambda}}[D-H + i\int_0^D \sigma(\tau)d\tau]}. \quad (28)$$

For boundary conditions (25) or (26), we have $r(\tilde{\lambda}) = 1$ or

$$r(\tilde{\lambda}) = \frac{a - i\sqrt{k_2^2 - \tilde{\lambda}}[1 + i\sigma(D)]}{a + i\sqrt{k_2^2 - \tilde{\lambda}}[1 + i\sigma(D)]}, \quad (29)$$

respectively. Notice that as $|a| \rightarrow \infty$, the boundary condition (26) is reduced to (25) and $r(\tilde{\lambda})$ converges to 1. Since $\sigma(z) = 0$ for $z \leq H$, Eq. (23) is simplified to

$$\rho \frac{d}{dz} \left(\frac{1}{\rho} \frac{d\tilde{\Phi}}{dz} \right) + k^2\tilde{\Phi} = \tilde{\lambda}\tilde{\Phi} \quad \text{for } 0 < z < H. \quad (30)$$

Therefore, the original PML eigenvalue problem (23), (24) with (25) or (26) is reduced to a nonlinear eigenvalue problem on a smaller interval: (30), (24) and (27). Notice that the only difference between the original and the PML eigenvalue problems is the boundary condition at $z = H$.

Let $\lambda \neq k_2^2$ be an eigenvalue of the original problem (19-21), we establish a perturbation result for $\tilde{\lambda}$ assuming that $|\varepsilon(\lambda)| \ll 1$, where the function ε is defined in (28). Although for a given waveguide and a given PML, the nonlinear eigenvalue problem (30), (24) and (27) can be solved by a numerical method, the perturbation result gives a useful explicit relationship between the PML parameters and $\tilde{\lambda}$.

Multiply equations (30) and (19) by $\rho^{-1}\phi$ and $\rho^{-1}\tilde{\Phi}$, respectively, and integrate from $z = 0$ to $z = H$, we obtain

$$q(\tilde{\lambda}) - i\sqrt{k_2^2 - \tilde{\lambda}} = (\tilde{\lambda} - \lambda) \int_0^H \frac{\rho(H)\phi(z)\tilde{\Phi}(z)}{\rho(z)\phi(H)\tilde{\Phi}(H)} dz.$$

To the leading order, $\tilde{\Phi} \approx \phi$ (up to a constant). A Taylor series of q around λ gives rise to

$$\tilde{\lambda} - \lambda = \frac{q(\lambda) - i\sqrt{k_2^2 - \lambda}}{F - q'(\lambda)} + O(\varepsilon^2),$$

where

$$F = \int_0^H \frac{\rho(H)\phi^2(z)}{\rho(z)\phi^2(H)} dz.$$

Since $q(\lambda)$ and $q'(\lambda)$ are still related to $\varepsilon(\lambda)$, we can simplify the above and obtain

$$\tilde{\lambda} - \lambda = \frac{-4(k_2^2 - \lambda)r(\lambda)}{2iF\sqrt{k_2^2 - \lambda} - 1} \varepsilon(\lambda) + O(\varepsilon^2) \quad (31)$$

where $r(\lambda)$ follows the definition of $r(\tilde{\lambda})$ given earlier. For the more general PML with a real part in the coordinate stretching given in (7), the perturbation result can be easily obtained by replacing σ by $\sigma - i\gamma$.

To verify the above perturbation result, we consider a Pekeris waveguide given by

$$\begin{aligned} \rho &= \rho_1 = 1000 \text{ kg/m}^3, & \text{for } 0 < z < G \\ c &= c_1 = 1500 \text{ m/s}, & \text{for } 0 < z < G \\ \rho &= \rho_2 = 1700 \text{ kg/m}^3, & \text{for } z > G, \\ c &= c_2 = 1666.67 \text{ m/s}, & \text{for } z > G, \\ \omega &= 480, & G = 50 \text{ m}. \end{aligned}$$

Thus, the frequency is approximately 76.394 Hz. A PML is placed in $H < z < D$ where

$$H = 70 \text{ m}, \quad D = 80 \text{ m}. \quad (32)$$

The function σ is defined such that $\sigma(z) = 0$ for $z \leq H$ and

$$\sigma(z) = \frac{10t^3}{1+t^2}, \quad t = \frac{z-H}{D-H} \quad \text{for } z > H. \quad (33)$$

The Pekeris waveguide has two trapped modes given by

$$\lambda_1^{(trap)} = 9.9794 \times 10^{-2}, \quad \lambda_2^{(trap)} = 9.1597 \times 10^{-2}$$

and an infinite sequence of leaky modes. The first two leaky modes are

$$\begin{aligned} \lambda_1^{(leak)} &= 7.8000 \times 10^{-2} + 1.7270 \times 10^{-3}i, \\ \lambda_2^{(leak)} &= 5.4287 \times 10^{-2} + 4.3156 \times 10^{-3}i. \end{aligned}$$

Table 1 : Exact (left column) and approximate (right column) of two trapped modes and the first two leaky modes of a Pekeris waveguide terminated by a PML.

$\tilde{\lambda}$	(31)
9.9795E-2 - 4.8227E-7i	9.9795E-2 - 4.8235E-7i
9.1607E-2 + 3.0579E-6i	9.1607E-2 + 3.1054E-6i
7.8435E-2 + 1.2133E-3i	7.8802E-2 + 1.3989E-3i
5.4385E-2 + 4.2507E-3i	5.4389E-2 + 4.2539E-3i

Next, we calculate a few modes for the Pekeris waveguide truncated with a PML together with the simple zero Dirichlet boundary condition (25). These results and the perturbation results from (31) are compared in Table 1. We observe that $\tilde{\lambda}$ is complex, even when the original λ is real (which corresponds to a trapped mode). This is undesirable, since it implies that the corresponding PML mode will decay or grow exponentially along the waveguide. For this example, these side-effects are negligible. When the two trapped modes are propagated over a range of 10 km, the first mode will gain a 0.77% in its magnitude and the second mode will lose about 5% in its magnitude. The second column in Table 1 is the perturbation result (31). Notice that our perturbation result gives a good prediction to the small imaginary part of $\tilde{\lambda}$ (when λ is real). The exact and perturbation results for the first two leaky modes are also listed in Table 1. A perturbation result for the eigenfunction $\tilde{\phi}$ is presented in the Appendix.

From (31), we observe that the difference between λ and $\tilde{\lambda}$ is on the order of ϵ . This means that the imaginary part of the horizontal wavenumber of the perturbed mode (for the waveguide terminated by a PML) is also on the order of ϵ . For the standard PML given in (2), the magnitude of ϵ is determined by the decay rate of the original mode in the homogeneous bottom and where the PML is terminated, i.e. D . If the original trapped mode is near cut-off, we can expect that the side-effect of the PML is large. Fortunately, we can use the real part γ in the complex coordinate stretching (7) to reduce the magnitude of the ϵ further. For the benchmark wedge problem, the number of trapped modes decreases as r is increased. If we only use the standard PML, large error will be introduced for r near those critical values where the number of trapped modes changes.

5 Conclusions

In this paper, using the benchmark wedge problem described in Jensen and Ferla (1990), we demonstrated that the PML is a very effective technique for terminating the unbounded ocean-bottom in one-way modeling of sound wave propagation in ocean. For waveguide problems, the distance along the waveguide axis is large and the small side effect introduced by a PML may lead to large errors. Existing theory of PML based on the reflection coefficient is not adequate for waveguide problems. We carried out a perturbation analysis for normal modes in waveguides truncated by a PML. Notice that a PML can cause a trapped mode to decay or grow along the waveguide axis, therefore, it is incorrect to call PML an absorbing layer. The accuracy of the perturbation results are illustrated in comparisons with the exact solutions. With the real part γ of the complex coordinate stretching given in (7), the side effect of a truncated PML can be reduced. We believe that the PML technique can be used for simulating wave propagations in extremely long waveguides, including those more realistic models with natural attenuation. The perturbation results developed in this paper can be used to estimate the side effects of the PML and to help choosing the PML parameters.

Acknowledgement: This research was partially supported by a City University of Hong Kong research grant (Project No. 7001289).

Appendix: a perturbation result on eigenfunctions

A perturbation result for the eigenfunction $\tilde{\phi}$ can also be established. Let $\tilde{\phi} = \phi + \epsilon v + O(\epsilon^2)$ and define the operator $\mathcal{L} = \rho \partial_z (\rho^{-1} \partial_z \cdot) + k^2(z) - \lambda$, we have

$$\begin{aligned} \mathcal{L}v &= s\phi \quad \text{for } 0 < z < H, \\ v &= 0 \quad \text{at } z = 0, \\ \frac{dv}{dz} - i\sqrt{k_2^2 - \lambda}v &= sF\phi(H) \quad \text{at } z = H. \end{aligned}$$

The function v can be written as $v = v_0 + w$, where v_0 is any function satisfying the following three conditions:

$$v_0 = 0 \quad \text{at } z = 0, \quad (34)$$

$$\frac{dv_0}{dz} - i\sqrt{k_2^2 - \lambda}v_0 = sF\phi(H) \quad \text{at } z = H, \quad (35)$$

$$\int_0^H \frac{1}{\rho} \phi \mathcal{L}v_0 dz = s \int_0^H \frac{1}{\rho} \phi^2 dz. \quad (36)$$

The last condition above is used to ensure that w has a solution, where w satisfies

$$\begin{aligned} \mathcal{L}w &= s\phi - \mathcal{L}v_0 \quad \text{for } 0 < z < H, \\ w &= 0 \quad \text{at } z = 0, \\ \frac{dw}{dz} - i\sqrt{k_2^2 - \lambda}w &= 0 \quad \text{at } z = H. \end{aligned} \tag{37}$$

For the fixed λ , consider the following associated linear eigenvalue problem:

$$\begin{aligned} \rho \frac{d}{dz} \left(\frac{1}{\rho} \frac{d\phi}{dz} \right) + k^2\phi &= \mu\phi, \quad 0 < z < H, \\ \phi(0) &= 0 \\ \phi'(H) - i\sqrt{k_2^2 - \lambda}\phi(H) &= 0. \end{aligned}$$

Let the eigenvalues and eigenfunctions be μ_j and ϕ_j for $j = 1, 2, \dots$, these eigenfunctions are ‘‘orthogonal’’ to each other:

$$\int_0^H \frac{1}{\rho} \phi_j \phi_k dz = 0, \quad \text{if } j \neq k.$$

Furthermore, we can assume that $\mu_1 = \lambda$ and $\phi_1 = \phi$, thus the right hand side of (37) can be expanded as

$$s\phi - \mathcal{L}v_0 = \sum_{j=2}^{\infty} c_j \phi_j,$$

where the coefficient of ϕ_1 is zero because of (36) and

$$c_j = - \frac{\int_0^H \frac{1}{\rho} \phi_j \mathcal{L}v_0 dz}{\int_0^H \frac{1}{\rho} \phi_j^2 dz}.$$

This gives rise to

$$w = \sum_{j=2}^{\infty} \frac{c_j}{\mu_j - \lambda} \phi_j.$$

One way to construct a function v_0 is to let

$$\frac{1}{\rho} \frac{dv_0}{dz} = A + Bz$$

for some constants A and B . From (34), we have

$$v_0(z) = \int_0^z (A + B\tau)\rho(\tau)d\tau.$$

The other two conditions (35) and (36) give rise to the following linear system:

$$\begin{bmatrix} c_{11} & c_{12} \\ c_{21} & c_{22} \end{bmatrix} \begin{bmatrix} A \\ B \end{bmatrix} = \begin{bmatrix} sF\phi(H) \\ -s \int_0^H \rho^{-1} \phi^2(z) dz \end{bmatrix},$$

where

$$\begin{aligned} c_{11} &= \rho(H) - i\sqrt{k_2^2 - \lambda} \int_0^H \rho(\tau)d\tau, \\ c_{12} &= H\rho(H) - i\sqrt{k_2^2 - \lambda} \int_0^H \tau\rho(\tau)d\tau, \\ c_{21} &= \int_0^H \frac{\phi(z)}{\rho(z)} [k^2(z) - \lambda] \left[\int_0^z \rho(\tau)d\tau \right] dz, \\ c_{22} &= \int_0^H \frac{\phi(z)}{\rho(z)} [k^2(z) - \lambda] \left[\int_0^z \tau\rho(\tau)d\tau \right] dz \\ &\quad - \int_0^H \phi(z) dz. \end{aligned}$$

References

Arnold A.; Ehrhardt, M. (1998): Discrete transparent boundary conditions for wide angle parabolic equations in underwater acoustics, *J Comput Phys*, vol. 145, no. 2, pp. 611–638.

Berenger, J. P. (1994): A Perfectly matched layer for the absorption of electromagnetic-waves, *J Comput Phys*, vol. 114, no. 2, pp. 185–200.

Chen, B.; Fang, D. G.; Zhou, B. H. (1995): Modified Berenger PML Absorbing boundary-condition for FD-TD meshes, *IEEE Microwave and Guided Wave Letters*, vol. 5, no. 11, pp. 399–401.

Chew, W. C.; Weedon, W. H. (1994): A 3D perfectly matched medium from modified Maxwells equations with stretched coordinates, *Microwave and Optical Technology Letters*, vol. 7, no. 13, pp. 599–604.

Chui, S. L.; Lu, Y. Y. (2004): A propagator- θ beam propagation method, *IEEE Photon Technol Lett*, vol. 16, no. 3, pp. 822–824.

Collins, M. D. (1990): Benchmark calculations for higher-order parabolic equations, *J Acoust Soc Am*, vol. 87, no. 4, pp. 1535–1538.

Collins, M. D. (1993a): An energy-conserving parabolic equation for elastic media, *J Acoust Soc Am*, vol. 94, no. 2, pp. 975–982.

Collins, M. D. (1993b): A split-step Padé solution for the parabolic equation method, *J Acoust Soc Am*, vol. 93, no. 4, pp. 1736–1742.

- Collins, M. D.; Westwood, E. K.** (1991): “A higher-order energy-conserving parabolic equation for range-dependent ocean depth, sound speed, and density”, *J Acoust Soc Am*, 89(3), 1068-1075, 1991.
- deSanto, J. A.** (1992): *Scalar Wave Theory – Green’s Functions and Applications*, Springer Verlag, New York.
- Evans, R. B.** (1983): A coupled mode solution for acoustic propagation in a waveguide with stepwise depth variations of a penetrable bottom, *J Acoust Soc Am*, vol. 74, no. 1, pp. 188–195.
- Fang, J. Y.; Wu, Z. H.** (1995): Generalized perfectly matched layer – an extension of Berenger’s perfectly matched layer boundary condition, *IEEE Microwave and Guided Wave Letters*, vol. 5, no. 12, pp. 451–453.
- Frisk, G. V.** (1994): *Ocean and Seabed Acoustics: a Theory of Wave Propagation*, Prentice Hall, Englewood Cliffs, N.J.
- Greene, R. R.** (1984): The rational approximation to the acoustic-wave equation with bottom interaction, *J Acoust Soc Am*, vol. 76, no. 6, pp. 1764–1773.
- Ha, T.; Seo, S.; Sheen D.** (2006): Parallel iterative procedures for a computational electromagnetic modeling based on a nonconforming mixed finite element method, *CMES: Computer Modeling in Engineering & Sciences*, vol. 14, no. 1, pp. 57-76.
- Hassan, O.; Morgan, K.; Jones, J.; Larwood B.; Weatherill, N. P.** (2004): Parallel 3D time domain electromagnetic scattering simulations on unstructured meshes, *CMES: Computer Modeling in Engineering & Sciences*, vol. 5, no. 5, pp. 383-394.
- Ho, P. L.; Lu, Y. Y.** (2003): Improving the beam propagation method for TM polarization, *Opt Quantum Electron*, vol. 35, no. 4, pp. 507–519.
- Jensen, F. B.; Ferla, C. M.** (1990): Numerical-solutions of range-dependent benchmark problems in ocean acoustics, *J Acoust Soc Am*, vol. 87, no. 4, pp. 1499–1510.
- Jensen, F. B.; Kuperman, W. A.; Porter, M. B.; Schmidt, H.** (1994): *Computational Ocean Acoustics*, American Institute of Physics.
- Lu, Y. Y.** (1998): A complex coefficient rational approximation of $\sqrt{1+x}$, *Applied Numerical Mathematics*, vol. 27, no. 2, pp. 141–154.
- Lu, Y. Y.; Ho, P. L.** (2002a): A single scatter improvement for beam propagation methods, *IEEE Photon Technol Lett*, vol. 14, no. 8, pp. 1103–1105.
- Lu, Y. Y.; Ho, P. L.** (2002b): Beam propagation method using a $[(p-1)/p]$ Padé approximant of the propagator, *Optics Letters*, vol. 27, no. 9, pp. 683–685.
- Milinazzo, F. A.; Zala, C. A.; Brooke, G. H.** (1997): Rational square-root approximations for parabolic equation algorithms, *J Acoust Soc Am*, vol. 101, pp. 760-766.
- Papadakis, J. S.; Taroudakis, M. I.; Papadakis, P. J.; Mayfield, B.** (1992): A new method for a realistic treatment of the sea bottom in the parabolic approximation, *J Acoust Soc Am*, vol. 92, no. 4, pp. 2030–2038.
- Porter, M. B.; Jensen, F. B.; Ferla, C. M.** (1991): The problem of energy-conservation in one-way models, *J Acoust Soc Am*, vol. 89, no. 3, pp. 1058–1067.
- Schmidt, F.; Friese, T.; Yevick, D.** (2001): Transparent boundary conditions for split-step Padé approximations of the one-way Helmholtz equation, *J Comput Phys*, vol. 170, no. 2, pp. 696–719.
- Tappert, F. D.** (1977): The parabolic approximation method, *Wave Propagation and Underwater Acoustics*, edited by J. B. Keller & J. S. Papadakis, Springer-Verlag.
- Thomson, D. J.** (1990): Wide-angle parabolic equation solutions to two range-dependent benchmark problems, *J Acoust Soc Am*, vol. 87, no. 4, pp. 1514–1520.
- Thomson, D. J.; Bohun, C. S.** (1988): A wide-angle initial field for parabolic equation models, *J Acoust Soc Am Suppl. 1*, vol. 83, pp. S118.
- Yevick, D.; Thomson, D. J.** (1999): Nonlocal boundary conditions for finite-difference parabolic equation solvers, *J Acoust Soc Am*, vol. 106, no. 1, pp. 143–150.
- Yevick, D.; Thomson, D. J.** (2000a): Impedance-matched absorbers for finite-difference parabolic equation algorithms, *J Acoust Soc Am*, vol. 107, no. 3, pp. 1226–1234.
- Yevick, D.; Thomson, D. J.** (2000b): Complex Padé approximants for wide-angle acoustic propagators, *J Acoust Soc Am*, vol. 108, no. 6, pp. 2784–2790.

Yevick D.; Yu, J.; Schmidt, F. (1997): Analytic studies of absorbing and impedance-matched boundary layers, *IEEE Photon Technol Lett*, vol. 9, no. 1, pp. 73–75.